Enhanced ultra violet resistance of epoxy nanocomposites filled with liquid-like graphene oxide/silicon dioxide nanofluid

Ruilu Yang, [iD] *[a] Qi Zhang,[a] Yaping Zheng, [iD] *[b] Jian Shi*[a] and Mengzhi Li[b]

The ultra violet (UV) resistance of epoxy resins has been paid more and more attention, and the development of highly efficient UV resistant materials is critical. Therefore, we showed liquid-like graphene oxide (GO)/silicon dioxide (SiO_2)-based derivatives for UV resistance of epoxy resins. To be specific, SiO_2 nanoparticles were deposited *in situ* on the surface of GO. Subsequently, a black, homogeneous and solvent-free GO/SiO_2 nanofluid was prepared by grafting organosilanes (KH560) and polyetheramines (M2070) on the surface of GO/SiO_2. Furthermore, the solvent-free GO/SiO_2 nanofluid/ epoxy resin composites were also prepared. The bending properties before and after UV irradiation of the nanocomposites at room temperature were investigated to reveal the role of the interphase. The toughening mechanism of GO/SiO_2 nanofluid was elucidated by observing the fracture surface. As expected, the loss of bending strength of the resin resulting from UV illumination was efficiently reduced by the GO/SiO_2 nanofluid. This may be attributed to the excellent anti-UV aging properties of GO and SiO_2 nanoparticles. Moreover, the GO/SiO_2 nanofluid can provide excellent bending resistance for epoxy resin both before and after illumination, owing to its great compatibility with epoxy resin by organic chains and hindrance to crack propagation by nano cores.

1. Introduction

As a kind of thermosetting engineering material, epoxy resin has been used in a wide range of applications in adhesives, coatings, electronic insulation, aerospace and especially for advanced composites, due to its excellent electrical insulation, great chemical stability, high thermal stability, and good mechanical performance.[1–4] Unfortunately, the brittleness and bending resistance of epoxy resin are deteriorated substantially after long-term ultraviolet radiation. This is because some of the chemical bonds of the epoxy resin can be broken by UV irradiation, leading to ageing and degradation of the epoxy resin.[5,6] As a result of this, aging leads to brittle fracture of equipment and materials, reducing the life of equipment and limiting the development of epoxy resins.

To overcome these limitations, various UV resistant nano materials such as TiO_2,[7] SiO_2,[8] carbon nanotubes (CNTs)[9] and graphene[10,11] were added into the epoxy resins. In particular, GO has many superior physical and chemical properties, owing to its single-layer planar membrane made of carbon atoms with sp^2 hybridized orbitals. Its high specific surface area, excellent heat conductivity and remarkable mechanical strength has attracted wide attention from industrial and academic fields.[12–14] Li *et al.*[15] produced a functional GO/epoxy nanocomposite coating using the chemical-bonding-dispersed approach. The material has multiple functions and long-term stability, which can be used for anticorrosion and weather resistance. The durability of the prepared nanocomposite under UV light was demonstrated by preventing the yellowing of the epoxy resin. Ferreira *et al.*[16] investigated the influence of amine-modified GO on the micro-hardness and dispersibility of epoxy-based nanocomposites. Fan *et al.*[17] alternately grafted rigid polydopamine PDA and flexible polyetheramine D230 on the surface of GO, allowing a "rigid-and-soft" multilayer interphase to be constructed between functionalized GO and epoxy matrix. The dispersion properties of GO in the epoxy matrix were researched.

At present, among the main methods for preparing GO/ epoxy nanocomposites, solution co-blending method has excellent dispersion effect, but it is easy to cause environmental pollution problems due to the organic solvents that is not easily removed.[18] The GO/epoxy nanocomposites prepared by *in situ* polymerization have good dispersion, but the polymerization viscosity is high when monomer and prepolymer are blended, which makes it difficult to operate.[19,20] Moreover, due to the high surface area and surface energy, the dispersion of GO in the resin matrix is not good by melt blending method.[21] Consequently, the solution of GO dispersion in epoxy resin matrix is a topic worthy of attention.

[a]Analysis and Testing Center, Nantong University, Nantong 226019, P. R. China. E-mail: yangruilu1987@126.com; shi.j1@ntu.edu.cn

[b]School of Chemistry and Chemical Engineering, Northwestern Polytechnical University, Xi'an 710072, P. R. China. E-mail: zhengyp@nwpu.edu.cn

Interestingly, recently, many researchers reported that grafting organic chains onto the surface of nanoparticles can effectively improve the agglomeration phenomenon of nanoparticles in epoxy resin, thereby increasing the mechanical, thermal and tribological performance of epoxy resin.[22–25] Compared with other nanomaterials, nanofluid materials have been widely applied in resin modification and reinforcement due to their unique properties, such as excellent compatibility, and their tailorability and functionality.[26,27] Guo *et al.*[28] prepared a new nanocomposite by homogeneously dispersing solvent-free ionic SiO₂ nanofluids into epoxy resin. The results show that the tribological performance of epoxy resin has been enhanced significantly by the addition of even low-loading SiO₂ nanofluids. Li *et al.*[29] prepared a nanocomposite by combining a solvent-free liquid-like nanocrystal-functionalized graphene oxide with epoxy resin. The impact toughness and glass transition temperature of neat epoxy were enhanced by 138.12% and 33.05 °C, respectively, at the 1.0 wt% fraction. Wang *et al.*[30] incorporated the prepared multiwalled carbon nanotube (MWNT) nanofluids into the epoxy resin matrix, and the bending strength, bending modulus and impact strength of nanocomposites containing 0.5 wt% MWNT increased by more than 10%, 14%, and 40%, respectively. Yao *et al.*[31] used a novel magnetic composite nanofluid as filler to improve the mechanical and thermal performances of epoxy resin. Wang *et al.*[32] designed a solvent-free nanofluids containing a multi-core of GO and Fe₃O₄ nanocrystalline to modify the damping and mechanical properties of epoxy. This nanofluid has the following advantages as the filler of epoxy resin: (1) *in situ* precipitation and organic chain surface modification can increase the spacing of GO lamellae and improve the dispersion of GO in epoxy resin; (2) due to the liquid phase and the amphipathicity of organic chain, the nanofluid material can be better mixed with the epoxy matrix to improve the dispersion of GO in the matrix. (3) The solvent-free state of nanofluid is friendly to the environment, maintaining zero vapor pressure at room temperature and ordinary pressure, and will not corrode equipment; (4) *in situ* deposition of UV-resistant nanoparticles on GO surface leads to a synergistic effect, thereby improving the UV-resistant aging performance of epoxy matrix. (5) The rigid GO and nanoparticles can prevent the silver grain from developing into cracks, meanwhile, the flexible organic chain can toughen the matrix. Consequently, the nanofluid can simultaneously strengthen and toughen the epoxy matrix.

Therefore, in this paper, SiO₂ nanoparticles were deposited *in situ* on the surface of GO. Subsequently, an organic long chain consisting of necked layer γ-(2,3-epoxypropoxypropyl) propyl trimethoxysilane and coronal layer polyetheramine 2070 was grafted on the surface of GO/SiO₂. Finally, the covalent GO/SiO₂ nanofluid were successfully prepared. Furthermore, the solvent-free GO/SiO₂ nanofluid/epoxy resin composites were also prepared. The bending properties and UV resistance of the nanocomposites at room temperature were investigated to reveal the role of interphase. The toughening mechanism of SiO₂/GO nanofluids was elucidated by observing the fracture surface.

Herein, the solvent-free GO/SiO₂ nanofluid was examined by spectroscopic and analytical TEM, FTIR, UV-Vis, XPS, TGA, and viscosity analyzes to precisely ascertain the solvent-free GO/SiO₂ nanofluid's various structural features. The solubility of GO/SiO₂ nanofluid in most polar solvents was also investigated. Most importantly, the bending strengths of the epoxy matrix with different contents of GO/SiO₂ nanofluid before and after UV illumination were analyzed and discussed. Furthermore, the toughening mechanism of SiO₂/GO nanofluids on epoxy matrix were discussed, by observing the SEM images of fractured surfaces of GO/SiO₂ nanofluid/epoxy composite before and after UV illumination.

2. Materials and methods

2.1. Materials

The graphite powder (<20 μm) was purchased from Xiamen Knanotech Port Co., Ltd, and prepared by mechanical exfoliation method. Trimethoxysilane (KH-560, 98 wt%) was provided by Chengdu aikeda chemicals Co., Ltd and etrabutyl titanate (TBOT, AR, ≧99%) was produced by Xi'an Fuchen Chemical Ind. Ltd (3-glycidyloxypropyl). Polyetheramine M-2070 ($M_w \sim$ 2000, Dalian Lianhao Inc., China) was used for polymeric canopy in this study. Other analytical reagents were purchased as follows from the Xi'an Fuchen Chemical Ind. Ltd, H₂SO₄, HCl, KMnO₄, H₂O₂, methanol, ethanol, glacial acetic acid, ammonia, acetone, tetrahydrofuran, toluene, trichloromethane and dimethyl formamide.

2.2. Synthesis of GO/SiO₂ nanofluid

As shown in Scheme 1, the synthesis process of GO/SiO₂ nanofluid. The modified Hummers' method[33] was used to prepare GO. Subsequently, 1 mg mL⁻¹ GO aqueous suspension was obtained under ultrasound. Then, the GO aqueous suspension in 50 mL was dispersed by ultrasonic and mixed with ethanol for 30 min. Meanwhile, some tetraethyl silicate was mixed with ethanol and glacial acetic acid and dispersed by ultrasonic for 30 min. Next, this tetraethyl silicate solution was added to the solution while stirring at room temperature while adding ammonia (25% aqueous solution) dropwise. After 12 h, the black floccule was observed in the solution. In order to remove the SiO₂ nanoparticles not deposited onto the surface of GO, the floccule was washed with distilled water for 3 times and
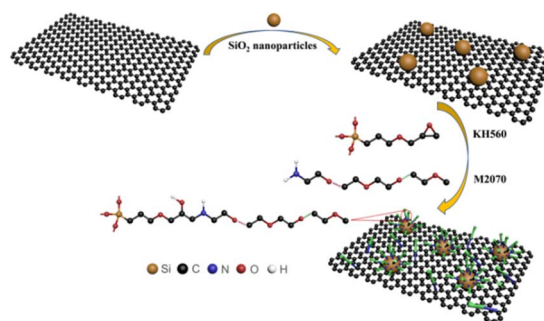
Scheme 1 The synthesis process of GO/SiO₂ nanofluid.

centrifuged at the speed of 8000 rpm for 15 min (Anke TGL-20B). Finally, GO/SiO$_2$ hybrid products were synthesized by freeze-drying the black floccule for 24 h.

To synthesize the nanofluids, first 5 mmol KH560 was added dropwise to a diluted solution of 5 mmol polyetheramine-M2070 (15 wt%), which was diluted with methanol and deionized water. After stirring at 45 °C for 12 h, the GO/SiO$_2$ mixture was added to the above solution. Then, under mechanical stirring, react at 25 °C for 5 h to guarantee full reaction. After that, the dialysis tubing (3.5k molecular weight cut-off) was used to remove the extra organic shell for 48 h and then the unreacted core was removed by centrifugation. In the end, the solvent was removed in a vacuum drying oven at 70 °C to gain the GO/SiO$_2$ nanofluid.

2.3. Preparation of GO/SiO$_2$ nanofluid/epoxy nanocomposites

At first, the GO/SiO$_2$ nanofluid was dispersed in epoxy resin (CYD-128) and curing agent (METHPA). Subsequently, the accelerating agent (DMP-30) was added to the above mixture, and then the mixture was stirred for 5 min. At last, the samples were cured at 90 °C for 30 min, then 110 °C for 30 min, 130 °C for 120 min and 150 °C for 60 min. To compare, pure epoxy composite without GO/SiO$_2$ nanofluid was also obtained in a similar way.

2.4. Characterization

Transmission electron microscope (TEM-H800, Hitachi Limited, Japan) was applied to investigate the microstructures and morphology of samples. The samples were obtained through dispersing samples in deionized water and collected on a copper grid. A WQF-310 FTIR spectrometer was used to conduct Fourier Transform Infrared (FTIR) analysis from 400 to 4000 cm^{-1}. Samples were measured with KBr pellet. The UV-vis absorption spectra were recorded with a Shimadzu UV2550 spectrometer in the range of 200–800 nm. Thermo Gravimetric Analysis (TGA) was measured with TGA Q50 TA instrument under N$_2$ flowing at a heating rate of 10 K min^{-1} from 25 to 800 °C. X-ray photoelectron spectra (XPS, Kratos Axis Ultra DLD) was applied to obtain the curves by placing some samples on a conductive blanket. The wide scan range is 0 to 1200 eV. The viscosity of the samples was measured with a Brookfield R/S plus Rotational Rheometer at a shear rate of 12.5° s^{-1} from 10 to 70 °C and a heating rate of 5 °C min^{-1}. TC-650 constant temperature water bath was used to stabilize the temperature. A universal testing machine (SANS, CMT-7205) was used to measure the bending mechanical properties of epoxy samples. Bending strength, namely flexural strength, is the ability of the material to withstand bending forces applied perpendicular to its longitudinal axis. The bending tests were performed based on GB/T 2567-2008 (Chinese Standard) under dry conditions. The sample size was $(80 \pm 0.02) \times (15 \pm 0.02) \times (3 \pm 0.02)$ mm^3. The bending strength was measured under a load peed of 2 mm min^{-1}. The pictures of fracture surface of samples after bending test were obtained by scanning electron microscope

(SEM, Hitachi S-4800) under 15 kV. The samples were previously coated with a conductive layer of gold.

The wavelength range of the UV lamp used in the UV treatment was 320–390 nm, and the intensity was 100 mW cm^{-2}. The front and back sides of the sample were irradiated for one hour respectively.

3. Results and discussion

Fig. 1 shows TEM images of GO, GO/SiO$_2$ hybrid and GO/SiO$_2$ nanofluid. In the image displayed in Fig. 1(a), the sheet structure and fold structure of GO is observed clearly. This observation indicates that the graphite is oxidized well. In addition, in the images shown in Fig. 1(b) and (c), the SiO$_2$ nanoparticles are dispersed on the surface of GO, and no agglomeration is observed in GO/SiO$_2$ nanofluid sample. This good dispersion is because the GO/SiO$_2$ nanofluid is wrapped with the layers of organic.

To further confirm that SiO$_2$ nanoparticles are deposited onto the surface of GO successfully, the FTIR spectra of GO, GO/SiO$_2$ hybrid and GO/SiO$_2$ nanofluid from 400–4000 cm^{-1} are collected and illustrated in Fig. 2(a). For GO, peaks at 3440 cm^{-1} and 1720 cm^{-1} are related to C=O and –OH vibrations from the acidic groups of GO.

Based on the report of Kou et al.[34] peaks at 1092 cm^{-1} and 465 cm^{-1} of GO/SiO$_2$ hybrid are originated from Si–O–Si asymmetric vibrations and bending vibrations, indicating that the SiO$_2$ nanoparticles are successfully deposited onto the surface of GO. In addition, for the GO/SiO$_2$ nanofluid, peaks at 2923 cm^{-1} and 2854 cm^{-1} are allocated to the vibrations of C–H,[35] which is the structure of M2070. Most importantly, the reaction of –NH$_2$ with the epoxy groups allows M2070 to bond with KH-560, which is demonstrated by the presence of –NH– at 1274 cm^{-1}. Furthermore, it can be seen that the spectra of the GO/SiO$_2$ nanofluid show remarkable bands at 1150 cm^{-1} and 840 cm^{-1}, related to Si–O–Si vibrations and O–Si–O vibrations, respectively. The results indicate that the SiO$_2$ nanoparticles are successfully deposited on the surface of GO, and the organic layer is successfully grafted onto the hybrid core surface, which are consistent with the results of TEM.

Fig. 2(b) shows the UV-Vis spectra of GO, GO/SiO$_2$ hybrid and GO/SiO$_2$ nanofluid. It has been noted that spectra of the GO exhibit remarkable band at 232 nm, which is associated with π–π* transition of C=C. Furthermore, for GO, absorption peak at 300 nm belongs to n → π* transition of C=O, indicating that the crystalline structure of graphite is destroyed by strong
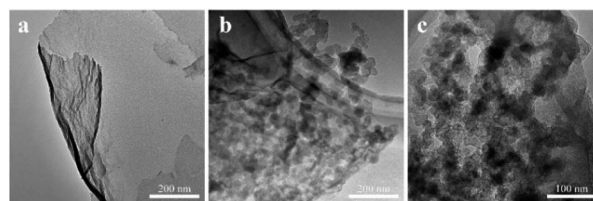

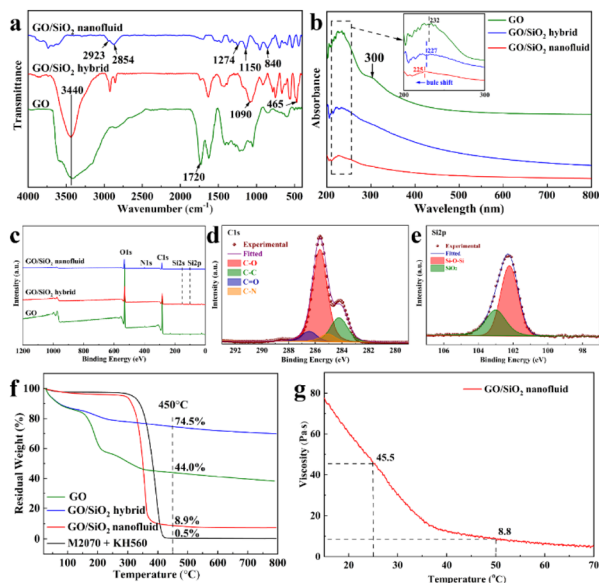**Fig. 1** TEM images of (a) GO, (b) GO/SiO$_2$ hybrid and (c) GO/SiO$_2$ nanofluid.

Fig. 2 (a) FTIR spectra of GO, GO/SiO$_2$ hybrid and GO/SiO$_2$ nanofluid, (b) UV-Vis spectra of GO, GO/SiO$_2$ hybrid and GO/SiO$_2$ nanofluid, (c) XPS spectra of GO, GO/SiO$_2$ hybrid and GO/SiO$_2$ nanofluid, (d) C 1s XPS spectra of GO/SiO$_2$ nanofluid, (e) Si 2p XPS spectra of GO/SiO$_2$ nanofluid, (f) TGA curves of GO, GO/SiO$_2$ hybrid, GO/SiO$_2$ nanofluid and organic layers (KH560 + M2070), (g) the viscosity of the GO/SiO$_2$ nanofluid from 10–70 °C.

oxidation.[36] Besides, as shown in Fig. 2(b) inset, the characteristic peak of GO at 232 nm also appears in the spectra of GO/SiO$_2$ hybrid and GO/SiO$_2$ nanofluid, with strong absorption at 227 and 225 nm, respectively. The peak shift from 232 nm to 227 and 225 nm is attributed to the introduction of SiO$_2$ and organic layers, which also result in the increase of the space steric hindrance an increase in spatial resistance. Consequently, the blue shift occurs as the degree of conjugation decreases and the molecular excitation wavelength shifts towards short-wave.

Illustrated in Fig. 2(c) are wide scan spectra of GO, GO/SiO$_2$ hybrid and GO/SiO$_2$ nanofluid. The peaks at 284, 400 and 532 eV correspond to C 1s, N 1s and O 1s, respectively. Furthermore, the appearance of Si 2s and Si 2p at 150 eV and 100 eV of GO/SiO$_2$ hybrid and GO/SiO$_2$ nanofluid confirm that SiO$_2$ nanoparticles are deposited onto the surface of GO. The result is consistent with that of FTIR and UV-Vis spectra. Furthermore, the high-resolution C 1s spectrum (Fig. 2(d)) displayed four C chemical forms of C–O, C=O, C–N and sp^2 C, which belong to 285.4 eV, 286.4 eV, 285.1 eV and 284.7 eV, respectively. In addition, the fitting peaks of high-resolution Si 2p spectrum were shown in Fig. 2(e), the peak positions at 102.2 eV and 103.0 eV are consistent with the Si–O–Si and SiO$_2$, respectively. This illustrates that the corona layers KH-560 have been grafted to the hybrid nanoparticles successfully.

The TGA curves of GO, GO/SiO$_2$ hybrid, GO/SiO$_2$ nanofluid and organic layers (KH560 + M2070) are illustrated in Fig. 2(f) to confirm the thermal stability and the content of the hybrid core in GO/SiO$_2$ nanofluid. A loss of weight is observed in both GO and GO/SiO$_2$ hybrid about 200 °C, owing to the decomposition of hydroxy, carboxyl and carbonyl of GO. However, it is noticed

that the rate of weight reduction of GO/SiO$_2$ hybrid is much lower than that of GO. This trend results from the great heat resistance of SiO$_2$ nanoparticles in GO/SiO$_2$ hybrid. In addition, it is clearly seen that the weights of GO/SiO$_2$ nanofluid barely changed below 300 °C, indicating that the GO/SiO$_2$ nanofluid has thermostability as reinforcing filler in resin, and is in a solvent-free, liquid-like state at room temperature. The long, flexible chains of the polyetheramine canopy contribute to this state. Furthermore, the TGA curve of KH560 + M2070 shows that there is a significant reduction in the weight of the sample in the range of 300–450 °C as a result of the decomposition of the organic layer. Subsequently, the weight of M2070 reaches 0.5% at 450 °C, indicating an almost complete decomposition of the organic shell in the range of 300–450 °C. Thereby, the GO/SiO$_2$ nanofluid remaining above 450 °C is SiO$_2$ nanoparticles, which is as high as 8.2 wt%.

The viscosity of the GO/SiO$_2$ nanofluid from 10–70 °C is demonstrated in Fig. 2(g). It is obviously observed that the temperature variation is having a significant impact on the viscosity of the GO/SiO$_2$ nanofluid. Particularly, the viscosity is decreasing while the temperature is increasing. This trend is because higher temperature leads to more active organic chains. In addition, it is illustrated in Fig. 2(g) that the viscosity of the GO/SiO$_2$ nanofluid is as high as 45.5 Pa s at room temperature, and as high as 8.8 Pa s at 50 °C. It can be concluded that the GO/SiO$_2$ nanofluid has good fluidity, whether at room temperature or higher temperature.

It is well known that the graphene nanosheets barely dissolved in most polar solvents. Fig. 3 investigates the solubility and dispersion of GO/SiO$_2$ nanofluid in water, some common organic solvents and the mixture of epoxy and MTHPA. It can be seen from image (a) that the GO/SiO$_2$ nanofluid homogeneously dispersed in these solvents. After one month, except in acetone and dimethylformamide, the GO/SiO$_2$ nanofluid still show good dispersion without precipitate in water and most organic solvents. This great dispersion of GO/SiO$_2$ nanofluid was provided by the oxygen groups on the organic chains of the nanofluid. The pure epoxy/MTHPA is shown in Fig. 3(b1) and the mixture of 1.0 wt% GO/SiO$_2$ nanofluid and epoxy/MTHPA is shown in Fig. 3(b2). As shown, the nanofluid is dispersed in the
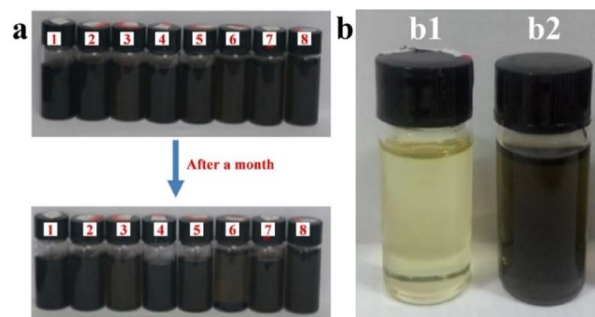

Fig. 3 (a) Solubility of GO/SiO$_2$ nanofluid in (1) water (2) ethanol (3) acetone (4) tetrahydrofuran (5) toluene (6) dimethyl formamide (7) trichloromethane and (8) methanol, (b) (b1) pure epoxy/MTHPA and (b2) epoxy/MTHPA with 1.0 wt% GO/SiO$_2$ nanofluid.

epoxy/MTHPA uniformly without stratification. The organic layer of the GO/SiO$_2$ nanofluid contains a large number of ether bonds and amino groups, which can be used as a curing agent with epoxy resin. So that, it has excellent dispersion in epoxy resin which containing a large number of ether bonds, hydroxyl groups and epoxy groups. It is well known that the dispersion of nanoparticles in the resins has a vital effect on the mechanical properties of resins. Therefore, the good dispersion brought by the organic layer of the GO/SiO$_2$ nanofluid has the potential to improve the mechanical properties of epoxy resins.

The bending strength of the epoxy resin with various content of GO/SiO$_2$ nanofluid was measured by the bending test. The results are shown in Fig. 4. The bending strength of pure epoxy resin is lower than that of the epoxy nanocomposite with the GO/SiO$_2$ nanofluid. The bending strength gradually increases with the increase content of GO/SiO$_2$ nanofluid when it is less than 0.8 wt%. This is due to the introduction of GO/SiO$_2$ nanofluid into the matrix. Firstly, the great compatibility between the organic layer of the GO/SiO$_2$ nanofluid and epoxy resin can enhance the mechanical properties of epoxy resin. Secondly, another reason for the increase in bending strength is usually that the toughness of epoxy resins is improved by the large surface area and high mechanical strength of GO and SiO$_2$. Furthermore, the GO/SiO$_2$ nanofluid shows fluid state without volatile solvent, so that there are no defects caused by bubbles during the curing process in epoxy resin. From the Fig. 4, the bending strength of the epoxy resin with 0.8 wt% GO/SiO$_2$ nanofluid is 136.34 MPa, which is 24.6% higher than that of pure epoxy. After that, the bending strength gradually decreased with the GO/SiO$_2$ nanofluid content increase. This phenomenon could be explained by the theory of silver stripes and shear bands, which could be induced at the interface of epoxy matrix and the nanoparticles by the cracks under the external forces. With increasing GO/SiO$_2$ nanofluid content in the epoxy matrix, the interface between the nanoparticles and the matrix also increases, and the induced silver stripes and shear bands become more, so that more energy can be absorbed by them. Therefore, the mechanical properties of the epoxy nanocomposite can be improved. But with GO/SiO$_2$ nanofluid
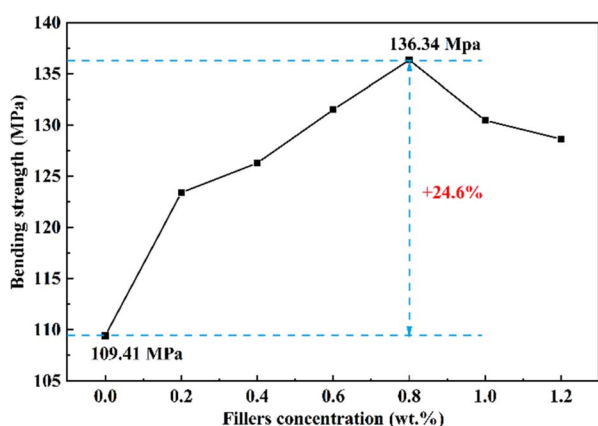
amount increasing, agglomeration of nanoparticles would happen. Under the external force, the material will be prone to larger silver stripes and plastic deformation, and eventually develop into macroscopic cracks which leading to decreasing of the epoxy nanocomposite performance. What's more, in Singh's research,[37] similar agglomeration effect at epoxy adhesive with metal decorated oxidized multiwalled carbon nanotube has been observed.

Illustrated in Fig. 5 are section images of pure epoxy matrix and epoxy nanocomposite with 0.8 wt% GO/SiO$_2$ nanofluid by SEM after bending test. The energy absorption of the materials during bending test were revealed by comparing the morphology of the two sections of samples. As shown in Fig. 5(a) and (b), it is a typical brittle fracture, because the fracture morphology of the pure epoxy matrix showed a smooth mirror-like fracture surface with river patterns. This can be ascribed to poor energy absorption during fracture resulting from the high cross-linking densities of pure epoxy matrix.[38] Thus, the pure epoxy matrix shows brittleness and low bending strength. Furthermore, Fig. 5(c) and (d) are fractography of epoxy matrix with 0.8 wt% GO/SiO$_2$ nanofluid. It is obvious from the SEM images that the surfaces of epoxy matrix with GO/SiO$_2$ nanofluid is coarser than that of the pure epoxy matrix. This is because the GO/SiO$_2$ nanofluid provides the material with the ability to prevent crack propagation. Therefore, hindrance to crack propagation results in coarse fracture surface and makes bending strength of the epoxy resin higher.

Fig. 6(a) shows the effect of different contents of GO/SiO$_2$ nanofluid on the bending strengths of the epoxy matrix before and after UV illumination. Consistent with the change in bending strength of samples before illumination, the bending strengths of all the samples after illumination also firstly
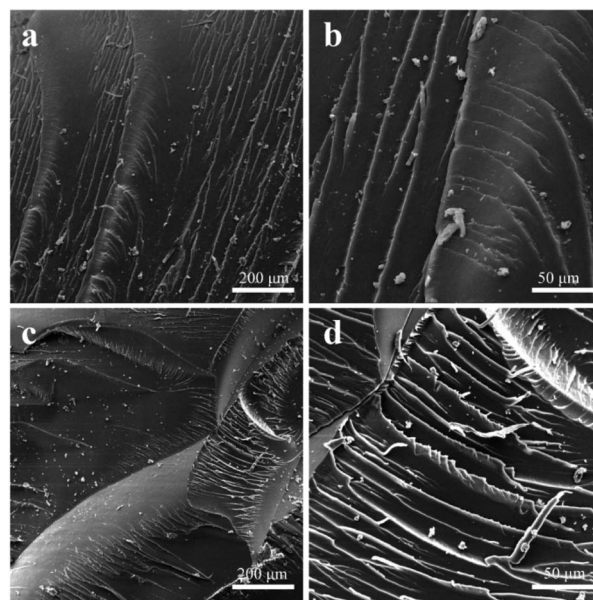

Fig. 4 Bending strength of the epoxy resin with different content of GO/SiO$_2$ nanofluid.

Fig. 5 SEM images of fractured surfaces of (a and b) neat epoxy, (c and d) GO/SiO$_2$ nanofluid/epoxy composite (0.8 wt%) before UV illumination.
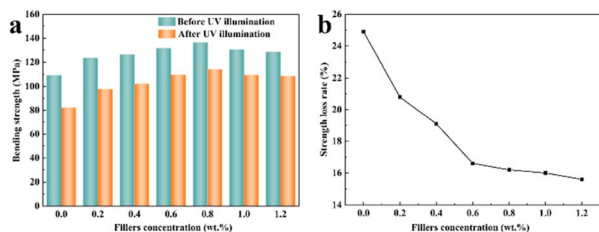
Fig. 6 (a) The bending strengths of the epoxy matrix with different contents of GO/SiO$_2$ nanofluid before and after UV illumination, (b) the strength loss rate of the composite with different contents of GO/SiO$_2$ nanofluid after UV illumination.

increased and then decreased as the increasing of GO/SiO$_2$ nanofluid content. Before and after illumination, maximum bending strengths of 136.34 MPa and 114.28 MPa were achieved, respectively, at 0.8 wt% GO/SiO$_2$ nanofluid. Furthermore, the bending strengths of pure epoxy resin decreased from 109.41 MPa before illumination to 82.12 MPa after illumination. The bending strengths of the composite with 0.8 wt% GO/SiO$_2$ nanofluid increased by 39.2% after illumination compared with the pure epoxy resin. Thus, the GO/SiO$_2$ nanofluid can provide excellent bending resistance for epoxy resin both before and after illumination, owing to its great compatibility with epoxy resin by organic chains and hindrance to crack propagation by nano core.

The strength loss rate of the composite with different contents of GO/SiO$_2$ nanofluid after UV illumination are depicted in Fig. 6(b). As evident from Fig. 6(b), with increasing GO/SiO$_2$ nanofluid content, the bending strength loss rates were reduced. A minimum bending strength of 15.6% was achieved at 1.2 wt% GO/SiO$_2$ nanofluid. Consequently, it can be concluded that GO/SiO$_2$ nanofluid can be used to effectively decrease the loss of bending strength of the resin due to UV illumination. This is attributed to the outstanding anti-UV aging property of GO and SiO$_2$ nanoparticles. Thus, increasing the content of GO/SiO$_2$ nanofluid can effectively reduce the amount of UV radiation absorbed by the epoxy resin.

To research further the fracture characteristics of epoxy resin after UV illumination, the fracture surface of pure epoxy resin and the epoxy resin with 0.8 wt% GO/SiO$_2$ nanofluid taken from bending tests were investigated by SEM. As depicted in Fig. 7, it is clear that the fracture surface of pure epoxy resin is smooth, mirror-like and river patterns, and it is a typical brittle fracture after UV illumination. Whereas, the epoxy resin with 0.8 wt% GO/SiO$_2$ nanofluid is covered with much rough and fluctuant lines with large and elongated crack pattern, suggesting that more bending energy can be dissipated through these lines.[39] These results indicate that GO/SiO$_2$ nanofluid can effectively enhance the bending strength of epoxy resin either before or after illumination, which is consistent with the bending test results.

From the above considerations, the toughening mechanism of the GO/SiO$_2$ nanofluid/epoxy resin composites before and after UV illumination can be proposed. Firstly, the GO/SiO$_2$ nanofluid shows fluid state without volatile solvent, so that
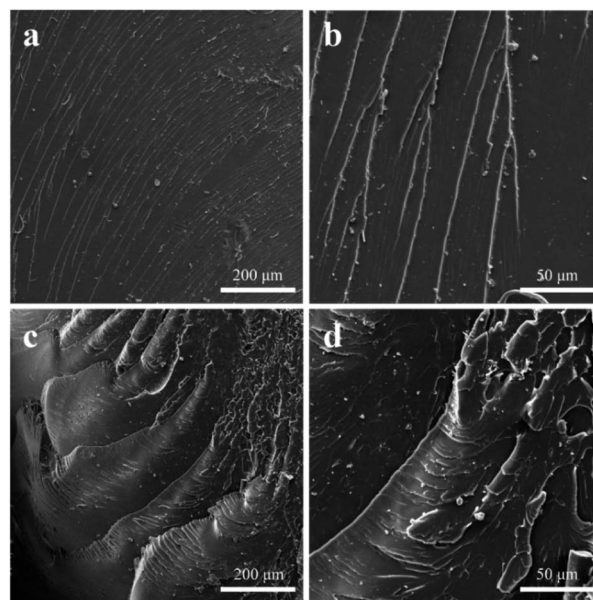

Fig. 7 SEM images of fractured surfaces of (a and b) neat epoxy, (c and d) GO/SiO$_2$ nanofluid/epoxy composite (0.8 wt%) after UV illumination.

there are no defects caused by bubbles during the curing process in epoxy resin, and the organic layer of the GO/SiO$_2$ nanofluid resulting in good compatibility with epoxy resin. All of this can enhance the mechanical properties of epoxy resin. Secondly, the toughness of epoxy resins is enhanced by the large surface area and high mechanical strength of GO and SiO$_2$. Most importantly, it could be induced at the interface of epoxy matrix and the nanoparticles by the cracks under the external forces. With increasing GO/SiO$_2$ nanofluid content in the epoxy matrix, the interface between the nanoparticles and the matrix also increases, and the induced silver stripes and shear bands become more, so that more energy can be absorbed by them. Therefore, the mechanical properties of the epoxy nanocomposite can be enhanced. Finally, the loss of bending strength of the resin resulting from UV irradiation was effectively reduced by GO/SiO$_2$ nanofluid. This is may be because of the great anti-UV aging property of GO and SiO$_2$ nanoparticles. Thus, the amount of UV radiation absorbed by the epoxy resin is reduced by the increase in GO/SiO$_2$ nanofluid content.

4. Conclusions

In the current study, a liquid-like GO/SiO$_2$ nanofluid for UV resistance of epoxy resins has been demonstrated by us. To be specific, SiO$_2$ nanoparticles were deposited *in situ* on the surface of GO. Then, the flexible oligomer species are formed by covalent bonding between organosilane (KH560) and polyether amine (M2070). Subsequently, the GO/SiO$_2$ mixture is able to flow at ambient temperature because of the oligomeric species. Furthermore, the solvent-free GO/SiO$_2$ nanofluid/epoxy resin composites were also prepared. The GO/SiO$_2$ nanofluid exhibited good solubility and dispersion in solvents and epoxy resins.

Most importantly, GO/SiO$_2$ nanofluid/epoxy resin composites showed excellent bending strength both before and after UV illumination due to its great compatibility with epoxy resin by organic chains and hindrance to crack propagation by nano cores. Compared to the neat epoxy, the incorporation of liquid-like GO/SiO$_2$ nanofluid/epoxy resin composites had been found to (1) increase the bending strength from 109.41 to 136.34 MPa, representing a 24.6% improvement at the 0.8 wt% fraction. Furthermore, the bending strengths of the composite containing 0.8 wt% GO/SiO$_2$ nanofluid increased by 39.2% after illumination compared with pure epoxy resin.

Author contributions

Ruilu Yang: formal analysis, investigation, writing – original draft, writing – review & editing, project administration; Qi Zhang: investigation, writing – original draft; Yaping Zheng: conceptualization, project administration, writing – review & editing; Jian Shi: supervision, writing – review & editing; Mengzhi Li: investigation.

Conflicts of interest

There are no conflicts to declare.

References

1 Y. Wang, S. Chen, X. Chen, Y. Lu, M. Miao and D. Zhang, *Composites, Part B*, 2019, **160**, 615–625.

2 J. C. Capricho, B. Fox and N. Hameed, *Polym. Rev.*, 2019, **60**, 1–41.

3 X. Mi, N. Liang, H. Xu, J. Wu, Y. Jiang, B. Nie and D. Zhang, *Prog. Mater. Sci.*, 2022, **130**, 100977.

4 B. Chen, Q. Wu, J. Li, K. Lin, D. Chen, C. Zhou, T. Wu, X. Luo and Y. Liu, *Chem. Eng. J.*, 2020, **379**, 122323.

5 M. M. Khotbehsara, A. Manalo, T. Aravinthan, J. Turner, W. Ferdous and G. Hota, *Polym. Degrad. Stab.*, 2020, **181**, 109352.

6 W. Xu, M. D. Eaton, S. Moreno-Da Silva and E. M. Perez, *RSC Adv.*, 2021, **11**, 36719–36725.

7 E. Rezvani Ghomi, S. Nouri Khorasani, M. S. Koochaki, M. Dinari, S. Ataei, M. H. Enayati, O. Das and R. Esmaeely Neisiany, *J. Adv. Res.*, 2023, **43**, 137–146.

8 J. Zheng, X. Zhang, J. Cao, R. Chen, T. Aziz, H. Fan and C. Bittencourt, *J. Appl. Polym. Sci.*, 2020, **138**, e50138.

9 W. Zhang, H. Cui, Y. Lv, Q. Yang, Y. Huang, G. Li and M. Kong, *J. Appl. Polym. Sci.*, 2022, **139**(26), e52457.

10 G.-G. Ying, C. Song, J. Ren, S.-Y. Guo, R. Nie and L. Zhang, *Constr. Build. Mater.*, 2021, **282**, 122644.

11 W. Yang, H. Ding, T. Liu, R. Ou, J. Lin, D. Puglia, P. Xu, Q. Wang, W. Dong, M. Du and P. Ma, *ACS Appl. Mater. Interfaces*, 2021, **13**, 59341–59351.

12 D. C. Marcano, D. V. Kosynkin, J. M. Berlin, A. Sinitskii, Z. Sun, A. Slesarev, L. B. Alemany, W. Lu and J. M. Tour, *ACS Nano*, 2010, **4**, 4806–4814.

13 D. R. Dreyer, S. Park, C. W. Bielawski and R. S. Ruoff, *Chem. Soc. Rev.*, 2010, **39**, 228–240.

14 B. Liu, J. Xie, H. Ma, X. Zhang, Y. Pan, J. Lv, H. Ge, N. Ren, H. Su, X. Xie, L. Huang and W. Huang, *Small*, 2017, **13**, 1601001.

15 Z.-J. Li, F.-S. Wang, Y.-C. Lai, Z.-E. Shi and Y.-H. Yu, *Prog. Org. Coat.*, 2021, **151**, 106052.

16 F. V. Ferreira, F. S. Brito, W. Franceschi, E. A. N. Simonetti, L. S. Cividanes, M. Chipara and K. Lozano, *Surf. Interfaces*, 2018, **10**, 100–109.

17 J. Fan, Z. Wang, J. Yang, X. Yin and Y. Zhao, *Appl. Surf. Sci.*, 2022, **585**, 152702.

18 M. Tomić, B. Dunjić, M. S. Nikolić, J. Maletaškić, V. B. Pavlović, J. Bajat and J. Djonlagić, *Appl. Clay Sci.*, 2018, **154**, 52–63.

19 W. B. Ying, H. S. Yang, D. S. Moon, M. W. Lee, N. Y. Ko, N. H. Kwak, B. Lee, J. Zhu and R. Zhang, *J. Appl. Polym. Sci.*, 2018, **135**, 45790.

20 H. Kishi, N. Kimura, R. Hara, K. Yamada, T. Kakibe, S. Matsuda, A. Fujita and H. Furui, *Polymer*, 2022, **241**, 124520.

21 T.-T. Wang, P. Huang, Y.-Q. Li, N. Hu and S.-Y. Fu, *Compos. Commun.*, 2019, **14**, 55–60.

22 W. Zhang, G. Song, J. Zhu, C. Wang, H. Zheng, B. Li, Z. Yu, X. Yang and L. Ma, *Compos. Commun.*, 2022, **34**, 101262.

23 X. Liang, X. Li, Y. Tang, X. Zhang, W. Wei and X. Liu, *J. Colloid Interface Sci.*, 2022, **611**, 105–117.

24 X. Tang, Y. Zhou and M. Peng, *ACS Appl. Mater. Interfaces*, 2016, **8**, 1854–1866.

25 S. Zhou, J. Yan, J. Chen, H. Yan, Y. Zhang, J. Huang, G. Zhao, Q. Zhang and Y. Liu, *J. Mater. Sci. Technol.*, 2023, **136**, 13–20.

26 Y. Wang, D. Yao and Y. Zheng, *Adv. Compos. Hybrid Mater.*, 2019, **2**, 608–625.

27 A. V. Karatrantos, C. Mugemana, L. Bouhala, N. Clarke and M. Kroger, *Nanomaterials*, 2022, **13**, 2.

28 Y. Guo, L. Zhang, F. Zhao, G. Li and G. Zhang, *Composites, Part B*, 2021, **215**, 108751.

29 P. Li, Y. Zheng, M. Li, T. Shi, D. Li and A. Zhang, *Mater. Des.*, 2016, **89**, 653–659.

30 Y. Wang, D. Wang, Z. He, D. Yao and Y. Zheng, *Polym. Compos.*, 2021, **42**, 3262–3271.

31 D. Yao, N. Peng and Y. Zheng, *Compos. Sci. Technol.*, 2018, **167**, 234–242.

32 Y. Wang, D. Yao, F. Su, D. Wang and Y. Zheng, *Mater. Lett.*, 2020, **274**, 127999.

33 Z. Zhang, R. Yang, Y. Zheng, H. Bai, J. Shi, J. Zhang, X. Zhou, M. Cai, S. Fan and C. Li, *Colloid Polym. Sci.*, 2021, **300**, 83–93.

34 L. Kou and C. Gao, *Nanoscale*, 2011, **3**, 519–528.

35 C. Zeng, Z. Tang, B. Guo and L. Zhang, *Phys. Chem. Chem. Phys.*, 2012, **14**, 9838–9845.

36 J. Chen, B. Yao, C. Li and G. Shi, *Carbon*, 2013, **64**, 225–229.

37 A. K. Singh, B. P. Panda, S. Mohanty, S. K. Nayak and M. K. Gupta, *J. Mater. Sci.: Mater. Electron.*, 2017, **28**, 8908–8920.

38 D. R. Bortz, E. G. Heras and I. Martin-Gullon, *Macromolecules*, 2011, **45**, 238–245.

39 P. Li, Y. Zheng, R. Yang, W. Fan, N. Wang and A. Zhang, *Chemphyschem*, 2015, **16**, 2524–2529.